ORIGINAL ARTICLE

Activated STING in a Vascular and Pulmonary Syndrome

Y. Liu, A.A. Jesus, B. Marrero, D. Yang, S.E. Ramsey, G.A. Montealegre Sanchez, K. Tenbrock, H. Wittkowski, O.Y. Jones, H.S. Kuehn, C.-C.R. Lee, M.A. DiMattia, E.W. Cowen, B. Gonzalez, I. Palmer, J.J. DiGiovanna, A. Biancotto, H. Kim, W.L. Tsai, A.M. Trier, Y. Huang, D.L. Stone, S. Hill, H.J. Kim, C. St. Hilaire, S. Gurprasad, N. Plass, D. Chapelle, I. Horkayne-Szakaly, D. Foell, A. Barysenka, F. Candotti, S.M. Holland, J.D. Hughes, H. Mehmet, A.C. Issekutz, M. Raffeld, J. McElwee, J.R. Fontana, C.P. Minniti, S. Moir, D.L. Kastner, M. Gadina, A.C. Steven, P.T. Wingfield, S.R. Brooks, S.D. Rosenzweig, T.A. Fleisher, Z. Deng, M. Boehm, A.S. Paller, and R. Goldbach-Mansky

ABSTRACT

BACKGROUND

The study of autoinflammatory diseases has uncovered mechanisms underlying cytokine dysregulation and inflammation.

METHODS

We analyzed the DNA of an index patient with early-onset systemic inflammation, cutaneous vasculopathy, and pulmonary inflammation. We sequenced a candidate gene, *TMEM173*, encoding the stimulator of interferon genes (STING), in this patient and in five unrelated children with similar clinical phenotypes. Four children were evaluated clinically and immunologically. With the STING ligand cyclic guanosine monophosphate–adenosine monophosphate (cGAMP), we stimulated peripheral-blood mononuclear cells and fibroblasts from patients and controls, as well as commercially obtained endothelial cells, and then assayed transcription of *IFNB1*, the gene encoding interferon-β, in the stimulated cells. We analyzed *IFNB1* reporter levels in HEK293T cells cotransfected with mutant or nonmutant STING constructs. Mutant STING leads to increased phosphorylation of signal transducer and activator of transcription 1 (STAT1), so we tested the effect of Janus kinase (JAK) inhibitors on STAT1 phosphorylation in lymphocytes from the affected children and controls.

RESULTS

We identified three mutations in exon 5 of *TMEM173* in the six patients. Elevated transcription of *IFNB1* and other gene targets of STING in peripheral-blood mononuclear cells from the patients indicated constitutive activation of the pathway that cannot be further up-regulated with stimulation. On stimulation with cGAMP, fibroblasts from the patients showed increased transcription of *IFNB1* but not of the genes encoding interleukin-1 (*IL1*), interleukin-6 (*IL6*), or tumor necrosis factor (*TNF*). HEK293T cells transfected with mutant constructs show elevated *IFNB1* reporter levels. STING is expressed in endothelial cells, and exposure of these cells to cGAMP resulted in endothelial activation and apoptosis. Constitutive up-regulation of phosphorylated STAT1 in patients' lymphocytes was reduced by JAK inhibitors.

CONCLUSIONS

STING-associated vasculopathy with onset in infancy (SAVI) is an autoinflammatory disease caused by gain-of-function mutations in *TMEM173*. (Funded by the Intramural Research Program of the National Institute of Arthritis and Musculoskeletal and Skin Diseases; ClinicalTrials.gov number, NCT00059748.)

The authors' full names and academic degrees are listed in the Appendix. The authors' affiliations are as follows: National Institute of Arthritis and Musculoskeletal and Skin Diseases (Y.L., A.A.J., B.M., G.A.M.S., M.A.D., I.P., H.K., W.L.T., A.M.T., Y.H., N.P., D.C., M.G., A.C.S., P.T.W., S.R.B., Z.D., R.G-M.), National Cancer Institute (C.-C.R.L., E.W.C., J.J.D., M.R.), National Heart, Lung, and Blood Institute (D.Y., A. Biancotto, C.S.H., J.R.F., C.P.M., M.B.), Department of Laboratory Medicine (H.S.K., S.G., S.D.R., T.A.F.), National Human Genome Research Institute (D.L.S., F.C., D.L.K.), Department of Radiology and Imaging Services (S.H.), National Institute on Deafness and Other Communication Disorders (H.J.K.), and National Institute of Allergy and Infectious Diseases (S.M.H., S.M.) — all at the National Institutes of Health (NIH), and Walter Reed National Military Medical Center (O.Y.J., I.H.-S.) — both in Bethesda, MD; Dalhousie University, Halifax, NS, Canada (S.E.R., A.C.I.); Rheinisch–Westfaelische Technische Hochschule Aachen, Aachen (K.T.), and University Hospital of Muenster, Muenster (H.W., D.F., A. Barysenka) — both in Germany; Luis Calvo Mackenna Hospital, Santiago, Chile (B.G.); Merck Research Laboratories, Boston (J.D.H., H.M., J.M.); and Northwestern University Feinberg School of Medicine, Chicago (A.S.P.). Address reprint requests to Dr. Goldbach-Mansky at the National Institute of Arthritis and Musculoskeletal and Skin Diseases, NIH Bldg. 10, Rm. 6D-47B, 10 Center Dr., Bethesda, MD 20892, or at goldbacr@mail.nih.gov.

Drs. Liu, Jesus, and Marrero, and Drs. Deng, Boehm, and Paller, contributed equally to this article.

STUDIES INVOLVING CHILDREN WITH MONO-genic autoinflammatory disease have provided insights into the regulation of key proinflammatory cytokine pathways and their role in causing systemic and organ-specific inflammation.[1,2] We studied six patients who presented in early infancy with systemic inflammation and violaceous, scaling lesions of fingers, toes, nose, cheeks, and ears that progressed to acral necrosis in most of the patients and did not respond to therapy. A mixed histologic pattern was observed, consisting of a prominent dermal inflammatory infiltrate with features of leukocytoclastic vasculitis and microthrombotic angiopathy of small dermal vessels. Three of the patients had severe interstitial lung disease.

Although many of the genetically defined autoinflammatory diseases are associated with increased interleukin-1 signaling and have a clinical response to interleukin-1 inhibition,[2] interleukin-1–inhibiting therapy was ineffective in one of the patients. A prominent interferon-response-gene signature in the peripheral blood of this participant suggested interferon dysregulation similar to that seen in other genetically defined inflammatory syndromes, including the Aicardi–Goutières syndrome,[3,4] an early-onset inflammatory encephalopathy, and chronic atypical neutrophilic dermatosis with lipodystrophy and elevated temperature (CANDLE),[5,6] a proteasome-associated autoinflammatory syndrome with proposed interferon-mediated pathologic features.[7,8] We detected autosomal dominant mutations in *TMEM173*, the gene encoding the stimulator of interferon genes (STING), in the six children we assessed, who presented with a clinical syndrome we have called STING-associated vasculopathy with onset in infancy (SAVI).

METHODS

PATIENTS

Written informed consent was provided for all four living study participants; for three participants, one or both parents provided written informed consent, and the fourth provided written informed consent himself. These patients were enrolled in an ongoing, institutional review board–approved study of the pathogenesis and natural history of their systemic inflammatory disease at the National Institutes of Health.

GENETIC STUDIES

We obtained samples of genomic DNA from Patient 1 and her parents for whole-exome sequencing (performed by Otogenetics and Beijing Genomics Institute). We used Sanger sequencing to analyze the introns and exons of *TMEM173*, the candidate gene revealed by means of whole-exome sequencing, in five unrelated patients who presented with a clinically similar phenotype.

FUNCTIONAL STUDIES

Quantitative reverse-transcriptase–polymerase-chain-reaction, cytokine, protein, and gene-expression analyses were performed according to standard procedures and are described in the Supplementary Appendix, available with the full text of this article at NEJM.org. Constructs of mutated *TMEM173* (V147L, N154S, V155M, and V155R) and nonmutated *TMEM173* were transfected into a STING-negative cell line (HEK293T cells) and stimulated with the STING ligand cyclic guanosine monophosphate–adenosine monophosphate (cGAMP [3′3′-cGAMP, Invivogen]).

When possible, we obtained blood and tissue samples from the study participants to assess activation and cell death of peripheral-blood cells. Tissue blocks from skin biopsies (in five patients), samples from lung biopsies (in two), and slides of a sample from a previous muscle biopsy (in one) were obtained and analyzed. Dermal fibroblast lines were obtained from two patients, four healthy controls, and three controls with the CANDLE syndrome. Primary endothelial cells were stimulated with the STING ligand cGAMP.

CD4 T cells and CD19 B cells from Patients 4 and 6 were treated for 4 hours with one of three Janus kinase (JAK) inhibitors — tofacitinib (1 μM), ruxolitinib (100 nM), or baricitinib (200 nM) — to assess their ability to block phosphorylation of the signal transducers and activators of transcription 1 (STAT1) and 3 (STAT3). Fibroblasts from Patient 1 and healthy controls were stimulated with 500 ng of cGAMP per milliliter and were also treated with 0.1 or 1.0 μM tofacitinib. We assayed the suppression of the gene encoding interferon-β (*IFNB1*) and other interferon-induced genes (*CXCL10*, *MX1*, and *OAS3*). Additional details are provided in the Supplementary Appendix.

RESULTS

CLINICAL PHENOTYPE

Demographic data and details of the clinical presentation of the six participants are provided in Table 1, and Table S1 in the Supplementary Appendix. All the patients were symptomatic within

the first 8 weeks of life. Two patients, Patients 1 and 5, presented initially with tachypnea. Between 2 weeks and 6 months of age, telangiectatic, pustular, or blistering rashes (or a combination of these types) developed on the cheeks, nose, fingers, toes, and soles of all the patients (Fig. 1A and 1B, and Fig. S1A through S1E in the Supplementary Appendix), with evidence of systemic inflammation (elevations of the erythrocyte sedimentation rate and C-reactive protein level) (Table S2 in the Supplementary Appendix). Five patients had recurrent low-grade fever flares. Skin lesions, which worsened in cold weather, extended to the pinnae of the ears and scattered sites on the extremities. Eschar and secondary painful crusts covered ulcerated skin lesions (Fig. S1A through S1E in the Supplementary Appendix).

Over time, clinical features of small-vessel damage developed in all the patients, including nailfold capillary tortuosity and capillary-loop loss (in three patients) (Fig. S1F and Table S1 in the Supplementary Appendix), and telangiectasia of the extremities and hard palate (in all six). Vascular occlusions caused scarring of the ear cartilage and perforation of the nasal septum (Fig. S1A, S1G, S1H, and S1I in the Supplementary Appendix), dystrophic nail changes, resorption of distal phalanges of fingers and toes, and gangrenous digits necessitating surgical amputation (Table 1; and Table S1 and Fig. S1C, S1D, S1J, S1K, and S1L in the Supplementary Appendix).

Samples from biopsies of lesional skin in all the patients revealed marked vascular inflammation limited to capillaries (Fig. 1C, and Fig. S2A through S2L in the Supplementary Appendix). Microthrombotic vascular changes were seen predominantly in biopsy samples from chronic skin lesions. We did not see vasculitis of medium-size or large vessels or deep venous thrombosis. Skin-biopsy samples from four patients showed evidence of IgM deposition in two patients and C3 deposition in scattered vessels with fibrin deposits in three, suggesting the presence of trapped immune complexes (Fig. S2E through S2H in the Supplementary Appendix). Three patients had low-titer autoantibodies that are seen in vasculitis (cytoplasmic and perinuclear antineutrophil cytoplasmic antibodies [c-ANCA and p-ANCA, respectively]) and the antiphospholipid syndrome (anticardiolipin antibodies and antibodies against B_2-glycoprotein), but these antibodies disappeared over time (Table S1 in the Supplementary Appendix).

Table 1. Demographic and Clinical Characteristics of Six Patients with SAVI.*	
Characteristic	No. of Patients
Age at presentation 1 day to 8 wk	6
Sex	
Female	3
Male	3
Symptom at initial presentation	
Rash	4
Tachypnea	2
Features of systemic inflammation	
Increased acute-phase reactant level†	6
Fever	6
Features of peripheral vascular inflammation	
Acral violaceous plaques	6
Nodules on face, nose, or ears	6
Distal ulcerative lesions with infarcts	6
Manifestations of vascular and tissue damage	
Nail dystrophy or loss	6
Gangrene of fingers or toes	4
Nasal-septum perforation	4
Pulmonary manifestations	
Paratracheal adenopathy	6
Abnormal pulmonary-function test	5
Interstitial lung disease observed on CT	5
Lung fibrosis	3
Low-titer autoantibodies	
Antinuclear antibody	3
Antiphospholipid antibodies‡	5
c-ANCA	1
No response or incomplete response to treatment	
Glucocorticoid	6
DMARD	6
Biologic agent§	6

* The term c-ANCA denotes cytoplasmic antineutrophil antibody, CT computed tomography, DMARD disease-modifying antirheumatic drug, and SAVI stimulator of interferon genes (STING)–associated vasculopathy with onset in infancy.
† Measurements for acute-phase reactants included the C-reactive protein level and the erythrocyte sedimentation rate.
‡ Autoantibody titers were only transiently positive (Table S1 in the Supplementary Appendix).
§ Biologic agents that elicited minimal clinical responses are listed in Table S1 in the Supplementary Appendix.

Five of the six patients (all except for Patient 4) had evidence of interstitial lung disease, and all had hilar or paratracheal lymphadenopathy as observed on computed tomography of the chest (Fig. 1D). However, Patients 3, 4, and 6 had no respiratory symptoms. Lung-biopsy samples from
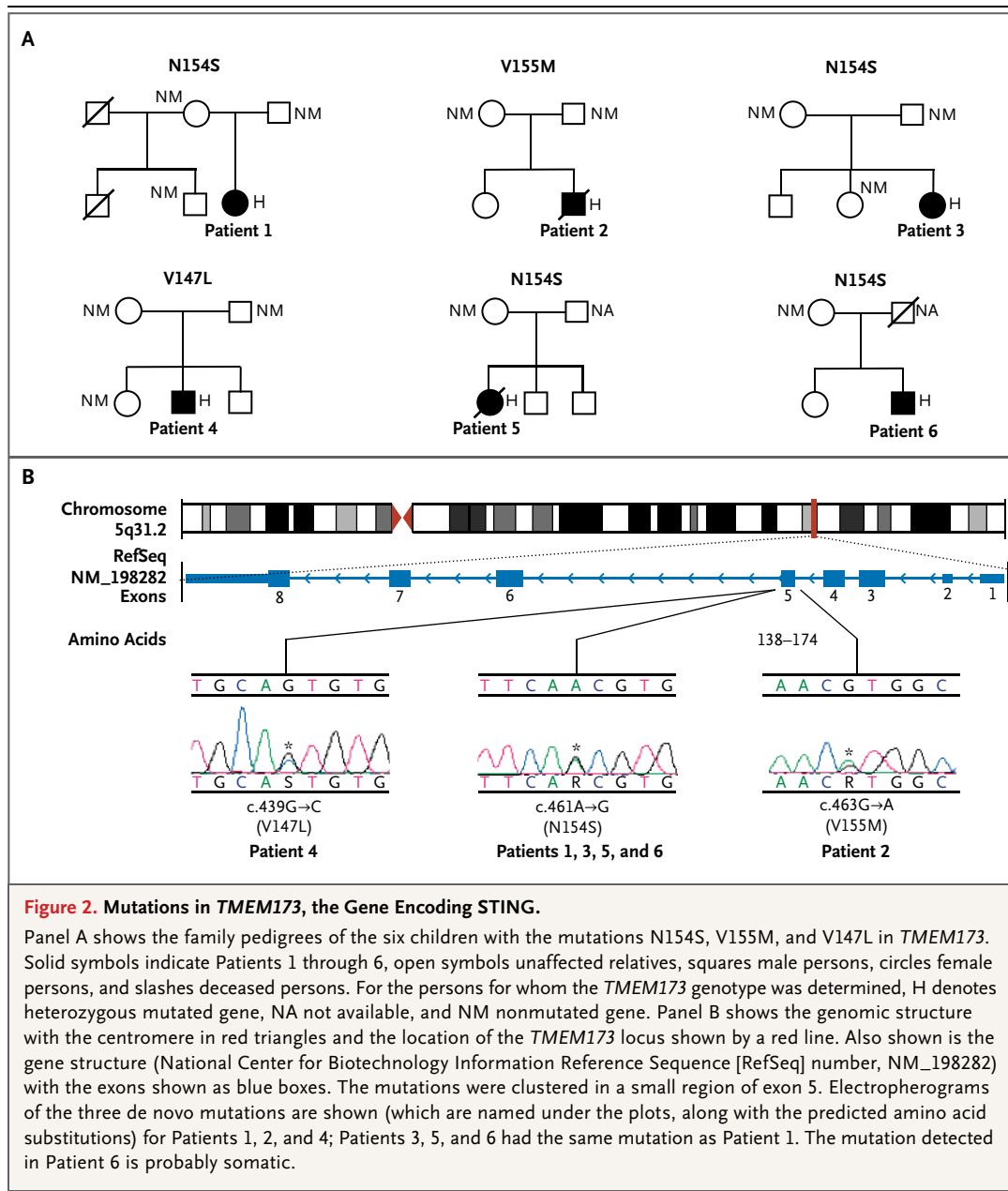
Figure 1. Clinical Features of Stimulator of Interferon Genes (STING)–Associated Vasculopathy with Onset in Infancy (SAVI).

Panel A shows the typical facial distribution of telangiectatic lesions on the nose and cheeks of Patient 1, who has SAVI. Panel B shows violaceous, scaling, atrophic plaques on the hands of Patient 6. Panel C shows histologic features of vascular inflammation in a skin-biopsy sample from a clinically involved area depicting a dense neutrophilic infiltrate with karyorrhexis throughout the vessel wall (hematoxylin and eosin); fibrin deposits are seen in the lumen of a severely damaged vessel. In Panel D, a high-resolution computed tomographic image of the lung of Patient 5 shows interstitial lung disease.

two patients (Patients 1 and 5) showed a scattered mixed lymphocytic inflammatory infiltrate (Fig. S3A through S3D in the Supplementary Appendix), interstitial fibrosis, and emphysematous changes (Fig. S3A in the Supplementary Appendix). All the patients had failure to thrive (Table S1 in the Supplementary Appendix).

By 7 years of age, Patient 5 had symmetric seropositive polyarthritis with carpal-bone erosions and progressive ulnar deviation (Fig. S1M in the Supplementary Appendix). Two patients (Patients 2 and 5) had histologically confirmed myositis and muscle atrophy (Fig. S3E and S3F in the Supplementary Appendix). These two chil-

Figure 2. Mutations in *TMEM173*, the Gene Encoding STING.

Panel A shows the family pedigrees of the six children with the mutations N154S, V155M, and V147L in *TMEM173*. Solid symbols indicate Patients 1 through 6, open symbols unaffected relatives, squares male persons, circles female persons, and slashes deceased persons. For the persons for whom the *TMEM173* genotype was determined, H denotes heterozygous mutated gene, NA not available, and NM nonmutated gene. Panel B shows the genomic structure with the centromere in red triangles and the location of the *TMEM173* locus shown by a red line. Also shown is the gene structure (National Center for Biotechnology Information Reference Sequence [RefSeq] number, NM_198282) with the exons shown as blue boxes. The mutations were clustered in a small region of exon 5. Electropherograms of the three de novo mutations are shown (which are named under the plots, along with the predicted amino acid substitutions) for Patients 1, 2, and 4; Patients 3, 5, and 6 had the same mutation as Patient 1. The mutation detected in Patient 6 is probably somatic.

dren died from pulmonary complications and secondary infection. An autopsy performed on Patient 2 showed a widespread vasculopathy of the systemic and pulmonary vasculature (Table S3 in the Supplementary Appendix).

GENETIC ANALYSIS OF *TMEM173* MUTATIONS

We performed whole-exome sequencing on samples from Patient 1 and her parents, and we filtered coding variants against allele frequencies from public and local databases and variants

found in her parents' samples. We identified a de novo germline mutation in a coding region of *TMEM173*, c.461A→G, p.N154S (Fig. 2, and Fig. S4A in the Supplementary Appendix). We used targeted Sanger sequencing of the candidate gene in five unrelated children with phenotypically similar disease. Three unrelated children, one of Turkish ancestry (Patient 3) and two of European ancestry (Patients 5 and 6), had the same mutation (p.N154S) as Patient 1, who is of French-Canadian ancestry. Samples from the

parents of Patients 1 through 4 and maternal samples available for Patients 5 and 6 were negative for the mutation.

Other de novo mutations were detected in Patient 2 (c.463G→A, p.V155M), who was of European ancestry, and Patient 4 (c.439G→C, p.V147L), who was of Chilean ancestry (Fig. 2B, and Fig. S4B and Table S4 in the Supplementary Appendix). Sanger sequencing of DNA from Patient 6 showed a variable prevalence of the mutation c.461A→G, p.N154S across different cell types (whole blood, neutrophils, buccal cells, dermal fibroblasts, and keratinocytes), suggesting somatic mosaicism of the mutation (Fig. S4B and S5 in the Supplementary Appendix). Amino acids at positions 154 and 155 were absolutely conserved across the STING orthologues (across a broad range of species) that we aligned (Fig. S6 in the Supplementary Appendix). The amino acid at position 147 was either valine or isoleucine in most of the STING orthologues we aligned, except for the chicken (*Gallus gallus*), which carries a leucine at amino acid position 147 (Fig. S6 in the Supplementary Appendix).

FUNCTIONAL ANALYSES

Constitutive Activation of the STING–Interferon-β Pathway

TMEM173 encodes the adaptor protein STING, which functions as a homodimer. On binding its ligand, cGAMP, it mediates the production of interferon-β by means of a pathway involving the phosphorylation of TANK-binding kinase 1 (TBK1) and interferon regulatory factor 3 (IRF-3) (Fig. 3).[9] The finding that all three mutations are predicted to result in the substitution of amino acid residues close to the STING dimerization site suggested that they might interfere with dimerization, but two recombinant mutant STING proteins (N154S and V155M) each formed a stable dimer (Fig. S7 in the Supplementary Appendix) (we did not carry out this experiment using the third mutation, V147L).

We observed a strong transcriptional interferon-response-gene signature and elevated levels of interferon-inducible protein 10 (IP-10) and other interferon-induced cytokines in the peripheral whole blood of four of the patients (Fig. 4A, and Table S5 in the Supplementary Appendix), suggesting that their *TMEM173* mutations effected a gain of function in STING, leading to overproduction of interferon. We used cGAMP to stimulate STING and then analyzed downstream events

in the STING–interferon-β pathway (IRF-3 phosphorylation and transcription of the gene encoding interferon-β [*IFNB1*]), interferon-induced STAT1 phosphorylation, and interferon-response-gene induction in participants' peripheral-blood mononuclear cells (PBMCs) and fibroblasts.

STING was expressed in T cells, monocytes, natural killer cells, and dermal fibroblasts but was absent in neutrophils and resting B cells (Fig. S8A and S8B in the Supplementary Appendix). Transcription of *IFNB1* and the induction of interferon-response genes were maximally upregulated in PBMCs from the patients; exposure to cGAMP brought about no change (Fig. 4B, and Fig. S8C in the Supplementary Appendix). In contrast, expression of *IFNB1* and interferon-response genes in control cells was low at baseline and increased on exposure to cGAMP. Baseline and induced transcription levels of the genes encoding interferon-α4 (*IFNA4*), interferon-γ (*IFNG*), and the proinflammatory cytokine interleukin-1β (*IL1B*) were similar in patients and controls, whereas transcription of the genes encoding tumor necrosis factor (*TNF*) and interleukin-6 (*IL6*) was elevated in unstimulated PBMCs from the patients and was augmented on exposure to cGAMP (Fig. S8C in the Supplementary Appendix).

STAT1 was constitutively phosphorylated in T and B lymphocytes from the three patients tested and could not be further increased with interferon-α stimulation. Phosphorylation of other STATs was also up-regulated either by interferon-β directly[10] or by other induced cytokines (Fig. S9A and S9B in the Supplementary Appendix). In dermal fibroblasts from the patients, basal *IFNB1* transcription was not up-regulated (in Patient 1), but a set of IRF-3–dependent genes that were induced by cGAMP in controls was constitutively upregulated in fibroblasts from Patient 1 (Fig. S10A and S10B in the Supplementary Appendix). Fibroblasts from the patients were more responsive to low-dose stimulation with cGAMP with upregulation of IRF-3 phosphorylation (Fig. S10C in the Supplementary Appendix) and *IFNB1* transcription than were fibroblasts from healthy controls or from patients with the CANDLE syndrome[6] (Fig. S10D and S10E in the Supplementary Appendix).

Transfection Experiments and Confirmation of Gain of Function

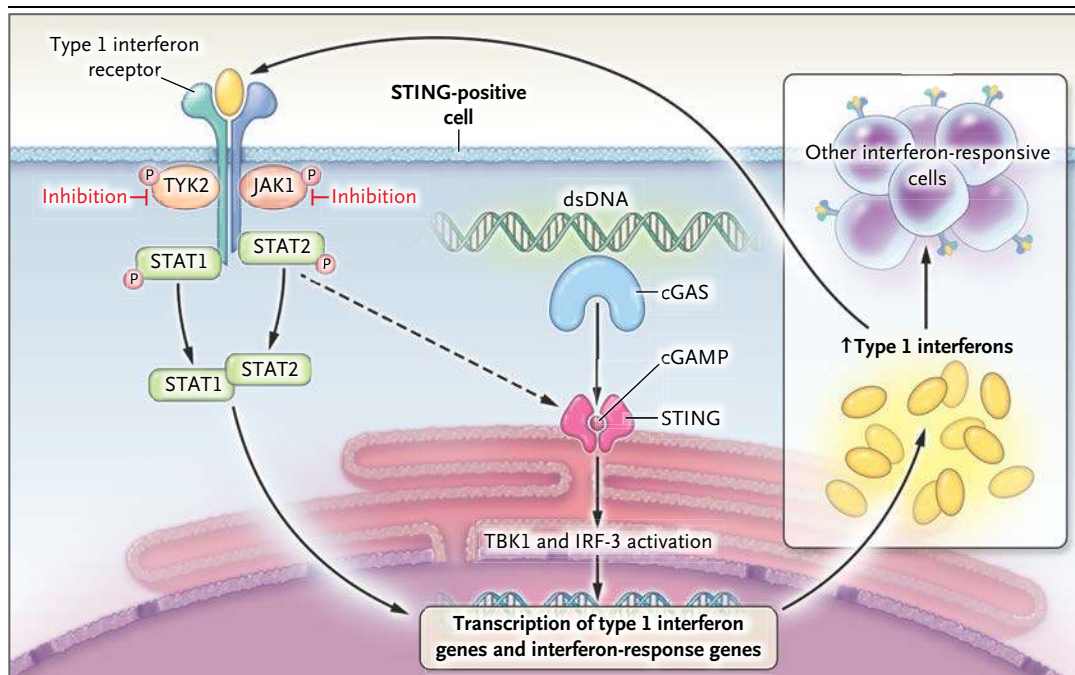We transfected HEK293T cells that do not express endogenous STING with nonmutant and

Figure 3. The STING–Interferon-β Pathway.

STING, an endoplasmic reticulum transmembrane protein, forms homodimers and functions as an adaptor for cytosolic DNA sensing. STING is activated by the binding of cyclic guanosine monophosphate–adenosine monophosphate (cGAMP), a second messenger that is synthesized by cyclic GMP–AMP synthase (cGAS), a family member of nucleotidyltransferases that is activated on its recognition and binding of double-stranded DNA (dsDNA). Binding of cGAMP to the STING homodimer activates interferon regulatory factor 3 (IRF-3) through TANK-binding kinase 1 (TBK1) and leads to the induction of interferon-β. In patients with SAVI, constitutively activated STING leads to increased transcription of the type 1 interferon gene, *IFNB1*, which encodes interferon-β. Binding of interferon-β to its receptor activates Janus kinases (JAKs), including JAK1 and tyrosine kinase 2 (TYK2), which in turn phosphorylate the receptor. This process allows the binding of the DNA-binding proteins signal transducers and activators of transcription 1 (STAT1) and 2 (STAT2) to the receptor, whereupon they become phosphorylated (P). Phosphorylation allows them to dimerize, and the dimer translocates to the nucleus, where it up-regulates transcription of interferon-response genes, including interferon regulatory factor 7–dependent transcription of type 1 interferon genes. The synthesis and release of interferons and their binding to interferon receptor further up-regulate STING and the transcription of other proinflammatory cytokine genes in a positive feedback loop. JAK inhibition blocks the loop, resulting in a decrease in STAT1 phosphorylation and transcription of its target genes in vitro.

mutant constructs encoding STING (N154S, V155M, and V147L, and a previously reported loss-of-function mutant, V155R).[11] *IFNB1* reporter activity was highly elevated in cells transfected with the three mutant constructs and was barely boosted on stimulation with the STING ligand cGAMP, a finding that was similar to our observations in PBMCs. In contrast, cells transfected with nonmutated *TMEM173*, *TMEM173* with the loss-of-function mutation, or control plasmid had no substantial baseline activation. Cells transfected with nonmutated *TMEM173* had a response to cGAMP stimulation in a dose-dependent manner, and the sample expressing the loss-of-function mutant had a minimal response only at the highest cGAMP concentration (Fig. 4C, and Fig. S11 in the Supplementary Appendix).

STING in Vasculitic Lesions and Its Activation in Endothelial Cells

STING was expressed in endothelial cells from biopsy samples of nonlesional skin from healthy adults and lesional skin from patients with SAVI and in commercially available endothelial-cell lines (Fig. S12A, S12B, and S13A in the Supplementary Appendix). It was also expressed in alveolar type 2 pneumocytes, bronchial epithelium, and alveolar macrophages in lung tissue (Fig. S12C through S12E in the Supplementary Appendix).

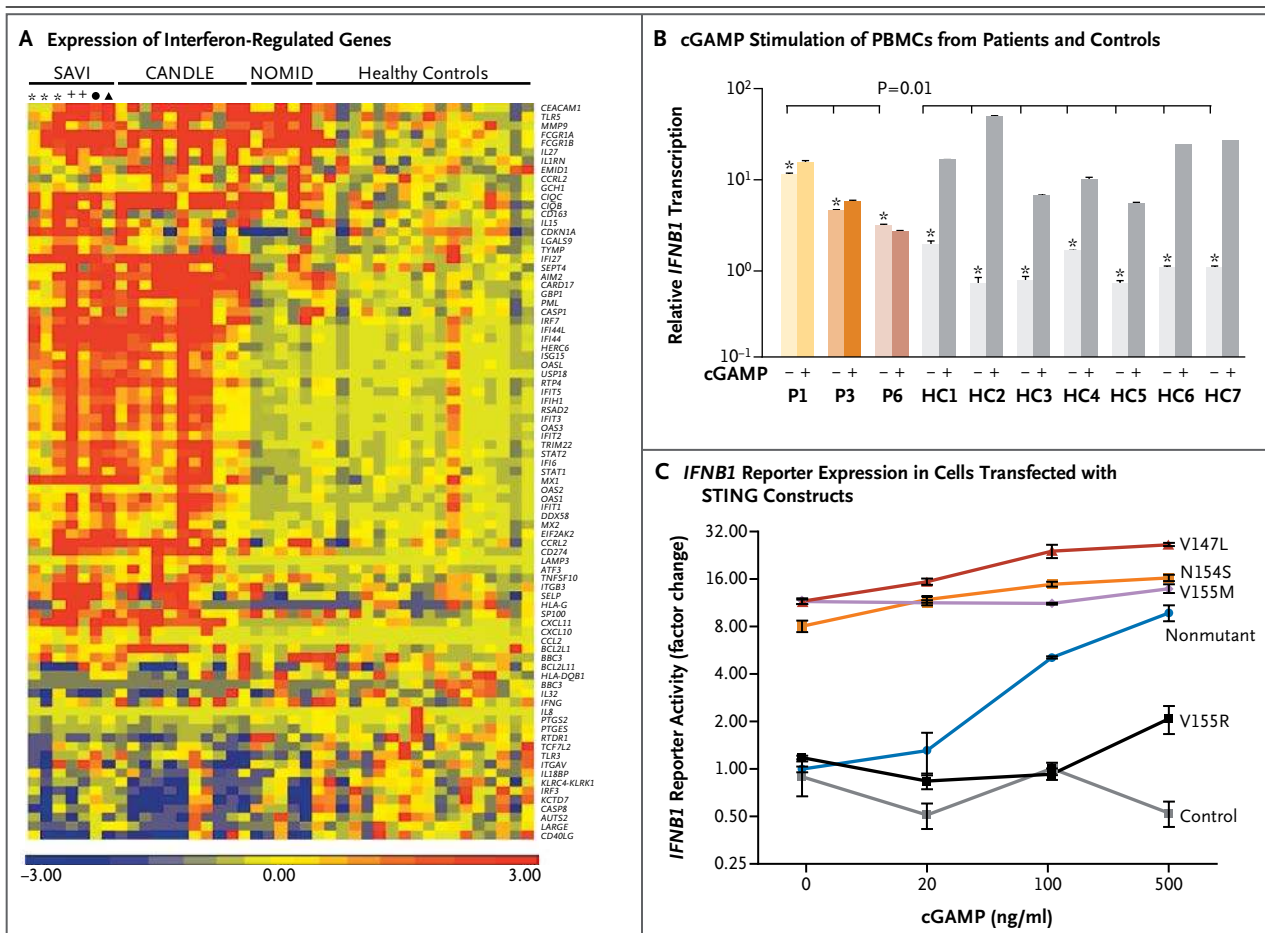Vascular endothelial cells in biopsy samples

A **Expression of Interferon-Regulated Genes**

B **cGAMP Stimulation of PBMCs from Patients and Controls**

C ***IFNB1* Reporter Expression in Cells Transfected with STING Constructs**

Figure 4. Functional Data Showing Gain-of-Function Mutation in *TMEM173* in Patients with SAVI.

In Panel A, a heat map shows increased expression of interferon-regulated genes in 4 patients with SAVI, as compared with another interferon-mediated autoinflammatory disease, the chronic atypical neutrophilic dermatosis with lipodystrophy and elevated temperature (CANDLE) syndrome (11 patients), the interleukin-1 mediated neonatal-onset multisystem inflammatory disease (NOMID; 5 patients), and 18 healthy controls. Up-regulated genes are shown in red, and down-regulated genes in blue. Asterisks indicate samples obtained at different time points from Patient 1, and plus signs indicate samples obtained at different time points from Patient 3. The circle indicates a sample from Patient 4, and the triangle a sample from Patient 6. Panel B shows the result of a quantitative reverse-transcriptase–polymerase-chain-reaction assay of *IFNB1* messenger RNA (mRNA) in peripheral-blood mononuclear cells (PBMCs) from 3 patients with SAVI and 7 relatives or controls, with (+) and without (−) cGAMP stimulation. Shown are normalized *IFNB1* mRNA levels against the average value for healthy controls in the absence of stimulation. P1, P3, and P6 denote Patients 1, 3, and 6, respectively. The healthy controls included Patient 1's sibling, father, and mother (HC1, HC2, and HC3, respectively), Patient 3's female sibling and mother (HC4 and HC5, respectively), and two persons who were unrelated to the patients (HC6 and HC7). Errors bars indicate the standard error for triplicates in the assay. Asterisks denote P=0.01 for the comparison between unstimulated samples from patients and unstimulated samples from controls; no significant increase in *IFNB1* mRNA levels was seen after cGAMP stimulation in the patients, as compared with controls. Panel C shows cotransfection of HEK293T cells with a *TMEM173* construct (2 ng of plasmid DNA), either the nonmutated gene or a gene with a disease-associated mutation (N154S, V155M, or V147L) or loss-of-function mutation (V155R), in addition to an *IFNB1* luciferase reporter construct, performed to assess *IFNB1* reporter activity with and without cGAMP stimulation. A green fluorescent protein expressing plasmid was also contransfected as control. The reporter activity was normalized to the result of nonmutant construct without cGAMP stimulation. The three constructs carrying the putative disease-causing mutations, but not the nonmutated constructs, constitutively activated *IFNB1* transcription, which was further up-regulated with cGAMP stimulation. The cells with the nonmutated construct responded to cGAMP stimulation in a dose-dependent manner, whereas the cells with the loss-of-function mutation V155R had minimal responses only at the highest cGAMP concentrations. The cells with the control transfection did not respond to all tested cGAMP concentrations. I bars indicate standard errors.

from lesional skin (from Patients 2 and 3) expressed selected markers of endothelial inflammation (inducible nitric oxide synthase), coagulation (tissue factor), and endothelial-cell adhesion and activation (E-selectin and intercellular adhesion molecule 1); we detected no up-regulation

of these markers in the endothelial cells of healthy controls. The endothelial-cell layer in affected vessels was damaged in some areas and was preserved in healthy controls (Fig. 5, and Fig. S13A in the Supplementary Appendix).

The skin-biopsy samples showed features of substantial cutaneous small-vessel inflammation with leukocytoclasia, which was present at an early stage of life in all the participants, leading to tissue loss on hands and feet (Fig. S1 and S2 in the Supplementary Appendix). Vasculopathic changes without evidence of thrombosis in larger vessels suggested a widespread vasculopathy (Table S3 in the Supplementary Appendix). To explore the effect of STING in endothelial-cell activation, we assessed the transcription profile of cGAMP-stimulated endothelial cells from human umbilical veins. The genes that showed the greatest increase in expression were interferon-response genes or other genes that mediate inflammation, as well as genes that control apoptosis, cell adhesion, and coagulation pathways (Fig. S13B and S13C in the Supplementary Appendix). Stimulation of endothelial cells with cGAMP led to increased expression of inducible nitric oxide synthase, E-selectin, and tissue factor and induced endothelial-cell death (Fig. S13D and S13E in the Supplementary Appendix). Spontaneous cell death was also observed in T cells and monocytes from the patients but not in B cells, which lack STING expression (Fig. S14 in the Supplementary Appendix).

Down-Regulation of STING–Interferon-β Pathway with JAK Inhibitors

There are currently no effective therapies for patients with this disease. We performed in vitro experiments to determine whether three JAK inhibitors — tofacitinib, ruxolitinib, and baricitinib — could suppress the expression of STING-induced targets and interferon-response genes.[12,13] The JAKs are activated by interferon receptors (on binding of interferon to the receptor) and phosphorylate the potent transcription factors STAT1 and STAT2, leading to the expression of interferon-response genes (Fig. 3).[14] Each of the JAK inhibitors blocked the constitutive phosphorylation of STAT1 in T cells and B cells from Patients 4 and 6 (Fig. 6, and Fig. S15A in the Supplementary Appendix). We observed a similar effect of tofacitinib on STAT3 phosphorylation in T cells from Patients 4 and 6 (Fig. S15B in the Supplementary Appendix). Treatment with a JAK inhibitor
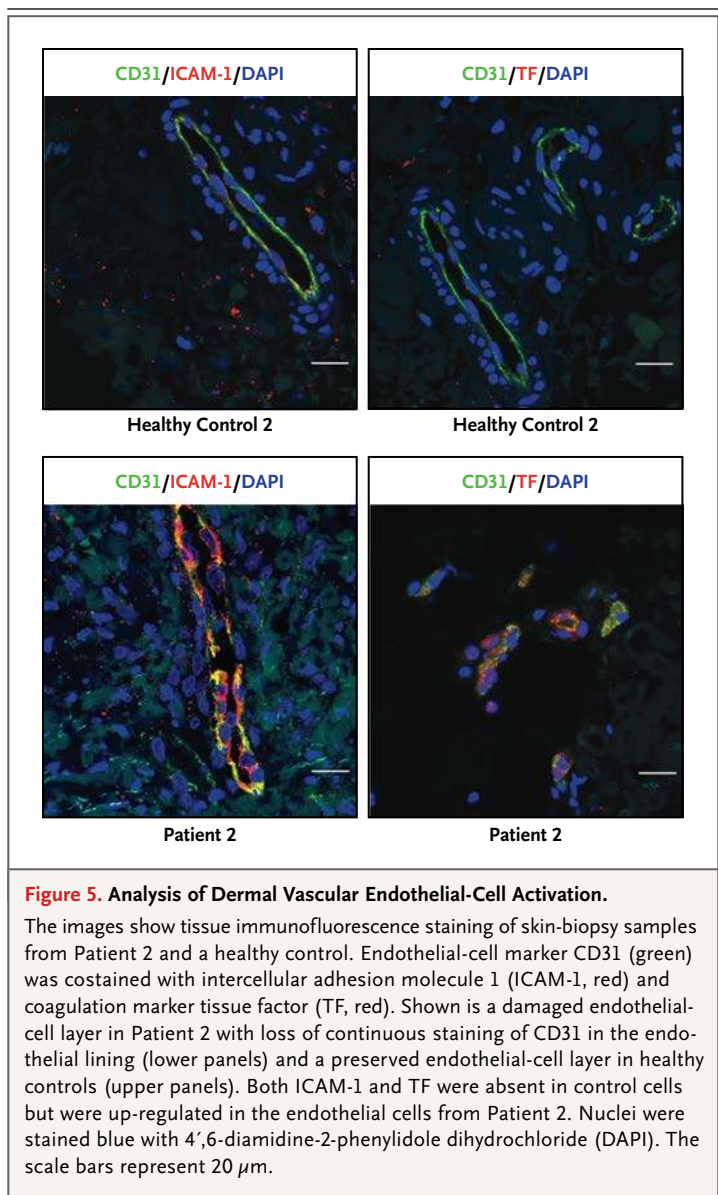

Figure 5. Analysis of Dermal Vascular Endothelial-Cell Activation.
The images show tissue immunofluorescence staining of skin-biopsy samples from Patient 2 and a healthy control. Endothelial-cell marker CD31 (green) was costained with intercellular adhesion molecule 1 (ICAM-1, red) and coagulation marker tissue factor (TF, red). Shown is a damaged endothelial-cell layer in Patient 2 with loss of continuous staining of CD31 in the endothelial lining (lower panels) and a preserved endothelial-cell layer in healthy controls (upper panels). Both ICAM-1 and TF were absent in control cells but were up-regulated in the endothelial cells from Patient 2. Nuclei were stained blue with 4′,6-diamidine-2-phenylidole dihydrochloride (DAPI). The scale bars represent 20 μm.

of fibroblasts from patients and controls that were then maximally activated with cGAMP led to a 30 to 50% reduction in *IFNB1* transcription and a 20 to 40% reduction in the transcription of *IL6* and *IL1B*. However, some interferon-response genes were blocked by 60 to 90% in a dose-dependent fashion (Fig. S16 in the Supplementary Appendix).

DISCUSSION

We describe a new autoinflammatory syndrome, which is caused by de novo mutations in *TMEM173*, the gene that encodes the STING pro-
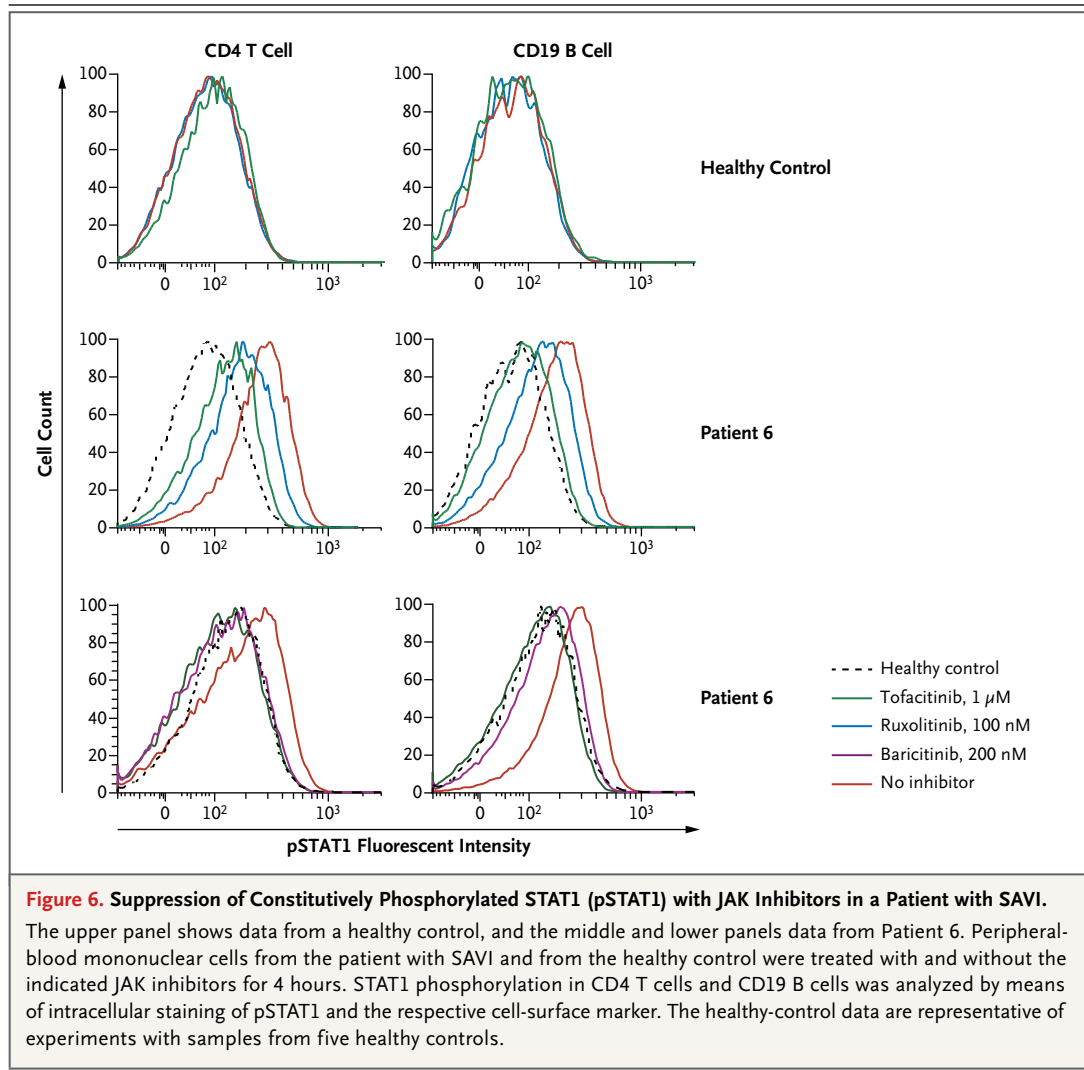
Figure 6. Suppression of Constitutively Phosphorylated STAT1 (pSTAT1) with JAK Inhibitors in a Patient with SAVI.

The upper panel shows data from a healthy control, and the middle and lower panels data from Patient 6. Peripheral-blood mononuclear cells from the patient with SAVI and from the healthy control were treated with and without the indicated JAK inhibitors for 4 hours. STAT1 phosphorylation in CD4 T cells and CD19 B cells was analyzed by means of intracellular staining of pSTAT1 and the respective cell-surface marker. The healthy-control data are representative of experiments with samples from five healthy controls.

tein. Our data suggest that the three *STING* mutations that we identified confer a gain of function and constitutive activation of STING and hypersensitivity to ligand stimulation, resulting in chronic activation of the STING–interferon pathway.

STING is a key adaptor molecule that links the sensing of cytosolic DNA, derived from foreign triggers (i.e., viral and bacterial) or from self, to the production of interferons,[15-19] which are potent cytokines with antiviral and antitumor activity.[20-22] Recently, the characterization of cyclic GMP–AMP synthase (cGAS) as a DNA sensor, which on binding double-stranded DNA releases the second messenger 2′3′-cGAMP (a high-affinity ligand of STING), has shed light on the mechanism of STING-induced interferon activation by means of TBK1 and IRF-3 phosphorylation.[23,24]

Interferons modulate innate (autoinflamma-

tory) and adaptive (autoimmune) pathologic immune responses in addition to the cell-intrinsic and antiviral effect.[25,26] Patients with SAVI share clinical, histologic, and functional features with patients who have the proteasome defect–associated autoinflammatory disease CANDLE,[5,6,27,28] the Aicardi–Goutières syndrome, or *TREX1*-mediated familial chilblain lupus.[29,30] Patients with these conditions have a vasculopathy early in life, have granulocyte precursors in the inflammatory skin infiltrate, and present with a prominent interferon-response-gene signature in the peripheral blood and with variable B-cell activation (Fig. S17 in the Supplementary Appendix), suggesting that different defects in the interferon pathway may result in overlapping clinical features.

The administration of recombinant interferon-α and interferon-β for the treatment of

chronic hepatitis and multiple sclerosis can, in rare cases, result in vasculitis,[31,32] and interferon-induced endothelial-cell dysfunction has been implicated as a cause of premature vascular damage and atherosclerosis in patients with systemic lupus erythematosus.[33] Nevertheless, the presentation of SAVI as an inflammatory vasculopathy was unexpected. The characteristic early onset and localized involvement of cheeks, ears, nose, and digits distinguish SAVI from other known vasculitis syndromes.[34] These features, antibodies associated with the antiphospholipid syndrome that were initially present at low titers and then disappeared, and the absence of thrombocytopenia also differentiate SAVI from typical presentations of the antiphospholipid syndrome.[35]

Stimulation of the STING pathway can activate endothelial cells directly and induces up-regulation of interferon-response genes, apoptosis-pathway genes, and endothelial-cell death in culture, as well as tissue-factor expression, which is a potent initiator of the coagulation cascade. Our data suggest that STING-induced endothelial-cell dysfunction may instigate an inflammatory and vaso-occlusive process and localize it to the vessels. In fact, the development of gangrene early in infancy in areas with low-flow circulation, such as the fingers, toes, nose, and ears, resembles other vaso-occlusive conditions characterized by activation of intravascular coagulation, including symmetric peripheral gangrene (a rare complication of sepsis),[36] the antiphospholipid syndrome,[37] and levamisole-induced vasculopathy,[38,39] raising questions about the role of STING-pathway dysregulation in these conditions.

Some studies have suggested that STING acts as a gatekeeper by streamlining the interferon signaling triggered by upstream double-stranded DNA sensors, such as cGAS.[15,40,41] For example, in a Trex1-deficient mouse model of the Aicardi–Goutières syndrome, the development of disease features depends on STING,[42] which suggests that the production of interferon in patients with the Aicardi–Goutières syndrome may depend on STING. Blocking STING may therefore represent an experimental therapeutic strategy in interferon-mediated diseases other than SAVI.[30]

Options for treating patients with SAVI are currently limited, but our study suggests that the blockade of interferon signaling with a JAK inhibitor may offer a therapeutic strategy. We observed that, at the right dose, JAK inhibitors blocked in vitro *IFNB1* transcription by 30 to 50% and the induction of interferon-response genes by 60 to 90%, suggesting that JAK inhibition may break a positive feedback loop that fuels continuous interferon signaling. A recently approved clinical protocol for the treatment of patients with SAVI will assess the clinical response to JAK inhibition (ClinicalTrials.gov number, NCT01724580).

APPENDIX

The authors' full names and academic degrees are as follows: Yin Liu, M.D., Ph.D., Adriana A. Jesus, M.D., Ph.D., Bernadette Marrero, Ph.D., Dan Yang, M.D., Ph.D., Suzanne E. Ramsey, M.D., Gina A. Montealegre Sanchez, M.D., Klaus Tenbrock, M.D., Helmut Wittkowski, M.D., Olcay Y. Jones, M.D., Ph.D., Hye Sun Kuehn, Ph.D., Chyi-Chia R. Lee, M.D., Ph.D., Michael A. DiMattia, Ph.D., Edward W. Cowen, M.D., Benito Gonzalez, M.D., Ira Palmer, M.S., John J. DiGiovanna, M.D., Angelique Biancotto, Ph.D., Hanna Kim, M.D., Wanxia L. Tsai, M.S., Anna M. Trier, B.A., Yan Huang, M.D., Deborah L. Stone, M.D., Suvimol Hill, M.D., H. Jeffery Kim, M.D., Cynthia St. Hilaire, Ph.D., Shakuntala Gurprasad, M.T., Nicole Plass, R.N., Dawn Chapelle, R.N., Iren Horkayne-Szakaly, M.D., Dirk Foell, M.D., Andrei Barysenka, Dipl.Phys., Fabio Candotti, M.D., Steven M. Holland, M.D., Jason D. Hughes, Ph.D., Huseyin Mehmet, Ph.D., Andrew C. Issekutz, M.D., Mark Raffeld, M.D., Joshua McElwee, Ph.D., Joseph R. Fontana, M.D., Caterina P. Minniti, M.D., Susan Moir, Ph.D., Daniel L. Kastner, M.D., Ph.D., Massimo Gadina, Ph.D., Alasdair C. Steven, Ph.D., Paul T. Wingfield, Ph.D., Stephen R. Brooks, Ph.D., Sergio D. Rosenzweig, M.D., Ph.D., Thomas A. Fleisher, M.D., Zuoming Deng, Ph.D., Manfred Boehm, M.D., Amy S. Paller, M.D., and Raphaela Goldbach-Mansky, M.D.

REFERENCES

1. Masters SL, Simon A, Aksentijevich I, Kastner DL. Horror autoinflammaticus: the molecular pathophysiology of autoinflammatory disease. Annu Rev Immunol 2009;27:621-68.
2. Sanchez GA, de Jesus AA, Goldbach-Mansky R. Monogenic autoinflammatory diseases: disorders of amplified danger sensing and cytokine dysregulation. Rheum Dis Clin North Am 2013;39:701-34.
3. Crow YJ. Aicardi-Goutières syndrome. Handb Clin Neurol 2013;113:1629-35.
4. Rice GI, Kasher PR, Forte GM, et al. Mutations in ADAR1 cause Aicardi-Goutières syndrome associated with a type I interferon signature. Nat Genet 2012;44:1243-8.
5. Agarwal AK, Xing C, DeMartino GN,

517

et al. PSMB8 encoding the β5i proteasome subunit is mutated in joint contractures, muscle atrophy, microcytic anemia, and panniculitis-induced lipodystrophy syndrome. Am J Hum Genet 2010;87:866-72.

6. Liu Y, Ramot Y, Torrelo A, et al. Mutations in proteasome subunit β type 8 cause CANDLE syndrome with evidence of genetic and phenotypic heterogeneity. Arthritis Rheum 2011;64:895-907.

7. Crow YJ. Type I interferonopathies: a novel set of inborn errors of immunity. Ann N Y Acad Sci 2011;1238:91-8.

8. Goldbach-Mansky R. Immunology in clinic review series: focus on autoinflammatory diseases: update on monogenic autoinflammatory diseases: the role of interleukin (IL)-1 and an emerging role for cytokines beyond IL-1. Clin Exp Immunol 2012;167:391-404.

9. Rani MR, Shrock J, Appachi S, Rudick RA, Williams BR, Ransohoff RM. Novel interferon-beta-induced gene expression in peripheral blood cells. J Leukoc Biol 2007;82:1353-60.

10. van Boxel-Dezaire AH, Zula JA, Xu Y, Ransohoff RM, Jacobberger JW, Stark GR. Major differences in the responses of primary human leukocyte subsets to IFN-beta. J Immunol 2010;185:5888-99.

11. Ouyang S, Song X, Wang Y, et al. Structural analysis of the STING adaptor protein reveals a hydrophobic dimer interface and mode of cyclic di-GMP binding. Immunity 2012;36:1073-86.

12. Rosengren S, Corr M, Firestein GS, Boyle DL. The JAK inhibitor CP-690,550 (tofacitinib) inhibits TNF-induced chemokine expression in fibroblast-like synoviocytes: autocrine role of type I interferon. Ann Rheum Dis 2012;71:440-7.

13. Clark JD, Flanagan ME, Telliez JB. Discovery and development of Janus kinase (JAK) inhibitors for inflammatory diseases. J Med Chem 2014 January 23 (Epub ahead of print).

14. O'Shea JJ, Holland SM, Staudt LM. JAKs and STATs in immunity, immunodeficiency, and cancer. N Engl J Med 2013; 368:161-70.

15. Zhang Z, Yuan B, Bao M, Lu N, Kim T, Liu YJ. The helicase DDX41 senses intracellular DNA mediated by the adaptor STING in dendritic cells. Nat Immunol 2011;12:959-65. [Erratum, Nat Immunol 2012;13:196.]

16. Keating SE, Baran M, Bowie AG. Cytosolic DNA sensors regulating type I interferon induction. Trends Immunol 2011; 32:574-81.

17. Burdette DL, Vance RE. STING and the innate immune response to nucleic acids in the cytosol. Nat Immunol 2013; 14:19-26.

18. Gall A, Treuting P, Elkon KB, et al. Autoimmunity initiates in nonhematopoietic cells and progresses via lymphocytes in an interferon-dependent autoimmune disease. Immunity 2012;36:120-31.

19. Ahn J, Gutman D, Saijo S, Barber GN. STING manifests self DNA-dependent inflammatory disease. Proc Natl Acad Sci U S A 2012;109:19386-91.

20. Isaacs A, Lindenmann J. Virus interference. I. The interferon. Proc R Soc Lond B Biol Sci 1957;147:258-67.

21. Stetson DB, Medzhitov R. Type I interferons in host defense. Immunity 2006; 25:373-81.

22. Kawai T, Akira S. The role of pattern-recognition receptors in innate immunity: update on Toll-like receptors. Nat Immunol 2010;11:373-84.

23. Wu J, Sun L, Chen X, et al. Cyclic GMP-AMP is an endogenous second messenger in innate immune signaling by cytosolic DNA. Science 2013;339:826-30.

24. Sun L, Wu J, Du F, Chen X, Chen ZJ. Cyclic GMP-AMP synthase is a cytosolic DNA sensor that activates the type I interferon pathway. Science 2013;339:786-91.

25. Trinchieri G. Type I interferon: friend or foe? J Exp Med 2010;207:2053-63.

26. Casanova JL, Holland SM, Notarangelo LD. Inborn errors of human JAKs and STATs. Immunity 2012;36:515-28.

27. Arima K, Kinoshita A, Mishima H, et al. Proteasome assembly defect due to a proteasome subunit beta type 8 (PSMB8) mutation causes the autoinflammatory disorder, Nakajo-Nishimura syndrome. Proc Natl Acad Sci U S A 2011;108:14914-9.

28. Kitamura A, Maekawa Y, Uehara H, et al. A mutation in the immunoproteasome subunit PSMB8 causes autoinflammation and lipodystrophy in humans. J Clin Invest 2011;121:4150-60.

29. Lee-Kirsch MA, Gong M, Schulz H, et al. Familial chilblain lupus, a monogenic form of cutaneous lupus erythematosus, maps to chromosome 3p. Am J Hum Genet 2006;79:731-7.

30. Rice G, Newman WG, Dean J, et al. Heterozygous mutations in TREX1 cause familial chilblain lupus and dominant Aicardi-Goutieres syndrome. Am J Hum Genet 2007;80:811-5.

31. Beuthien W, Mellinghoff HU, Kempis J. Vasculitic complications of interferon-alpha treatment for chronic hepatitis C virus infection: case report and review of the literature. Clin Rheumatol 2005;24:507-15.

32. Szilasiová J, Gdovinová Z, Jautová J, Baloghová J, Ficová M, Bohus P. Cutaneous vasculitis associated with interferon beta-1b treatment for multiple sclerosis. Clin Neuropharmacol 2009;32:301-3.

33. Denny MF, Yalavarthi S, Zhao W, et al. A distinct subset of proinflammatory neutrophils isolated from patients with systemic lupus erythematosus induces vascular damage and synthesizes type I IFNs. J Immunol 2010;184:3284-97. [Erratum, J Immunol 2010;185:3779.]

34. Jennette JC, Falk RJ, Bacon PA, et al. 2012 revised International Chapel Hill Consensus Conference Nomenclature of Vasculitides. Arthritis Rheum 2013;65:1-11.

35. Ruiz-Irastorza G, Crowther M, Branch W, Khamashta MA. Antiphospholipid syndrome. Lancet 2010;376:1498-509.

36. Goodwin JN. Symmetrical peripheral gangrene. Arch Surg 1974;108:780-4.

37. Thornsberry LA, LoSicco KI, English JC III. The skin and hypercoagulable states. J Am Acad Dermatol 2013;69:450-62.

38. Rongioletti F, Ghio L, Ginevri F, et al. Purpura of the ears: a distinctive vasculopathy with circulating autoantibodies complicating long-term treatment with levamisole in children. Br J Dermatol 1999;140:948-51.

39. Graf J. Rheumatic manifestations of cocaine use. Curr Opin Rheumatol 2013; 25:50-5.

40. Kondo T, Kobayashi J, Saitoh T, et al. DNA damage sensor MRE11 recognizes cytosolic double-stranded DNA and induces type I interferon by regulating STING trafficking. Proc Natl Acad Sci U S A 2013;110:2969-74.

41. Unterholzner L, Keating SE, Baran M, et al. IFI16 is an innate immune sensor for intracellular DNA. Nat Immunol 2010; 11:997-1004.

42. Stetson DB, Ko JS, Heidmann T, Medzhitov R. Trex1 prevents cell-intrinsic initiation of autoimmunity. Cell 2008;134: 587-98.